Progress in

PARTICLE AND NUCLEAR PHYSICS

Volume 2

Edited by

Sir Denys Wilkinson, F.R.S.

Progress in

PARTICLE AND NUCLEAR PHYSICS

Volume 2

(formerly Progress in Nuclear Physics)

Edited by

Sir Denys Wilkinson, F.R.S.
Vice-Chancellor, University of Sussex

PERGAMON PRESS

OXFORD · NEW YORK · TORONTO · SYDNEY · PARIS · FRANKFURT

U.K.	Pergamon Press Ltd., Headington Hill Hall, Oxford OX3 0BW, England
U.S.A.	Pergamon Press Inc., Maxwell House, Fairview Park, Elmsford, New York 10523, U.S.A.
CANADA	Pergamon of Canada, Suite 104, 150 Consumers Road, Willowdale, Ontario M2J 1P9, Canada
AUSTRALIA	Pergamon Press (Aust.) Pty. Ltd., P.O. Box 544, Potts Point, N.S.W. 2011, Australia
FRANCE	Pergamon Press SARL, 24 rue des Ecoles, 75240 Paris, Cedex 05, France
FEDERAL REPUBLIC OF GERMANY	Pergamon Press GmbH, 6242 Kronberg-Taunus, Pferdstrasse 1, Federal Republic of Germany

First Edition 1979

British Library Cataloguing in Publication Data

Progress in particle and nuclear physics.
Vol. 2
1. Particles (Nuclear physics)
I. Wilkinson, *Sir* Denys Haigh
539.7'21 QC793.2 79-40035

ISBN 0-08-023052-0

Printed and bound at William Clowes & Sons, Limited, Beccles and London

CONTENTS

LARGE TRANSVERSE MOMENTUM AND LARGE MASS PRODUCTION IN HADRONIC INTERACTIONS

C. MICHAEL

Department of Applied Mathematics and Theoretical Physics, University of Liverpool, P.O. Box 147, Liverpool L69 3BX, U.K.

CONTENTS

1. INTRODUCTION

In hadronic collisions, the average transverse momentum of the particles produced is limited, even at high energies. These small momentum-transfer mechanisms that are operating in hadron production will only be sensitive to the smeared properties of a hadron. This follows since small momentum corresponds to large distance in the usual quantum mechanical way. Effects of any detailed structure within hadrons and of any underlying constituents will not be apparent in such soft scattering processes.

Experimentally it is, however, possible to select events in which a large momentum is transferred to a hadron. These events are comparatively rare but can nevertheless be studied in considerable detail in contemporary experiments. Particularly well studied are many particle-production events at high energy in which one produced particle has a large transverse momentum relative to the incoming hadron directions. The spectrum of momentum of this one produced particle, disregarding all the others, is called the inclusive distribution or single particle-production distribution. This large transverse-momentum selection allows the possibility that short-distance behaviour within the hadrons may be resolved.

In order to probe short-distance behaviour, the large transverse-momentum particle must have been produced in a single large momentum-transfer process rather than in a succession of small momentum-transfer processes. This can be investigated experimentally by studying the momentum-transfer balance in the event. Thus a single large momentum-transfer subprocess will give rise to two particles with equal and opposite transverse momentum. A many-step mechanism, on the other hand, will result in the large transverse-momentum particle being balanced by many particles which share the transverse-momentum recoil among themselves.

Such simple criteria for a single hard scattering mechanism or a multiple soft scattering mechanism are unfortunately obscured by several effects. For a hard scattering subprocess, it is possible that the constituents that undergo the hard scattering are quarks (or antiquarks). The resultant large transverse-momentum quarks must then fragment to hadrons since no quarks are observed experimentally. This quark fragmentation gives rise to what is termed a jet. The jet is a collection of hadrons travelling in a similar direction. An example of a jet is the beam (or target) fragments in a typical hadronic collision. The data on e^+e^- annihilation to hadrons also shows evidence for two collinear hadronic jets in the final state. Thus rather than an isolated hadron at large transverse momentum, one may expect a group or jet of hadrons which can be thought of as fragments of the system produced in the hard scattering subprocesses. In the case of a many-step process producing large transverse momentum, the system produced may likewise fragment into several observed hadrons. One familiar example is the production of a resonance which then decays. As well as these extreme possibilities of single hard scattering and of multiple soft scattering, there are, of course, intermediate configurations. For example, the large p_T particle may be balanced by two systems which each carry a substantial fraction of the recoil. If the possibility that each of these systems fragment is included, this would yield three transverse jets in the final state.

Returning to the topic of elementary constituents inside a hadron, the primary evidence comes from using short-distance electromagnetic and weak currents as a probe. These data indicate that a hadron may be viewed as a distribution of constituents, or partons as they are called in this context. In short-distance phenomena, this distribution is sampled incoherently, so that a probability distribution of partons for different momenta may be defined. The quantum numbers carried by these partons are consistent with the assumption that they are quarks and antiquarks. A constituent which has no electromagnetic or weak interaction is also necessary and this is commonly identified with the gluons that provide binding between quarks.

The simplest approach to large p_T production in a parton framework is then to consider a hard (or elementary) scattering of a parton from one incoming hadron with a parton from the other incoming hadron. The resulting large transverse-momentum partons will then fragment into two jets. Data gives encouragement to this picture and many specific models have been developed. A discussion is given in Section 4.3. One of the crucial features is the nature of the parton–parton subscattering. This should be calculated from the underlying field theory.

The only class of field theories which reproduces the observed effects in current-induced short-distance phenomena is the class of asymptotically free theories. In these theories, the effective coupling of the constituents to each other become smaller as the distance scale decreases (and hence as the momentum scale increases). Thus, asymptotically in momentum, the constituents behave as free elementary particles and the parton distribution approach will be valid. The most attractive theory of quarks which is asymptotically free is quantum

chromodynamics (QCD). In QCD, the gluons are elementary massless vector particles which are in an octet representation of the SU(3) colour group. The quarks and antiquarks are coupled to these gluons and there are also explicit multiple gluon couplings. If only colour singlet states are assumed to be able to exist independently, the quarks and gluons are confined within hadrons. At present hadronic states cannot be calculated in this theory since only small-distance phenomena are amenable to calculation because the effective coupling is then weak. One of the main uses of QCD is to provide a field theoretic basis to the naïve parton model approach.

Returning to the parton–parton scattering subprocess, in QCD quark–quark elastic scattering (also $q\bar{q}$ elastic scattering) by one gluon exchange can be evaluated explicitly for large momentum transfers. The result is a dependence like p_T^{-4} on the transverse momentum p_T of the produced jet. This is in conflict with the observed single particle distribution which behaves more like p_T^{-8}. A range of corrections can be calculated and the QCD inspired estimate goes some way towards explaining the observed spectrum. This is discussed in Section 4.3.

A feature of some interest recently is the parton transverse momentum (k_T). In a naïve parton model approach, this should be small with $\langle k_T \rangle \sim 0.3\,\text{GeV}$. Considering hadron–hadron collisions in terms of a parton–parton subsystem scattering then implies that the parton–parton centre of mass can differ by $\sim k_T$ in transverse momentum from the hadron–hadron centre of mass. An analysis of data implies that $\langle k_T \rangle \sim 0.6\,\text{GeV}$ when so estimated from the distribution of the hard scattering centre of mass. In a field theoretic approach, such as QCD, such a relatively large value of k_T can be understood since additional large p_T gluons may always be produced and these simulate a large value of k_T. Put another way, the quark from the beam hadron which is going to partake in the hard scattering subprocess may first radiate gluons and this will modify its transverse momentum. These considerations are quite close to those conventional models for typical hadronic processes.

It is important to study average transverse momentum phenomena at the same time as large momentum phenomena in order to appreciate the differences. From the point of view of a field theory of elementary constituents, the surprise is not the presence of large transverse-momentum production processes, but rather the surprise is that the average transverse momentum is so small in hadronic collisions! Typical hadronic production can be visualized as a sort of bremmstrahlung of soft gluons in an approach such as QCD. These gluons then convert into quark–antiquark pairs which, in turn, recombine into colour singlet combinations to make mesons, some of which may subsequently decay to several mesons. This complicated scenario ensures that the mesons finally produced are almost independent of any underlying field theoretic production process. Indeed a statistical approach is very appropriate since so many degrees of freedom are available. Conventional models of hadronic production take no account of any elementary substructure and yield a p_T dependence which is a gaussian or an exponential.

Since experimentally there is no sharp transition between average p_T phenomena and large p_T phenomena, it is clearly desirable to have a model which bridges both régimes. One starting-point is a conventional hadronic production model which is modified to take account of the underlying field theoretic structure at short distance. As an example consider the independent emission of gluons. Soft gluons produced by small momentum-transfer processes will dominate as discussed above. There is always, however, the possibility of producing a large transverse momentum gluon with a probability which will depend on an inverse power of its transverse momentum. This large transverse momentum could either be

balanced by another large p_T gluon or by many soft gluons. In Section 3.2 a prototype model of this class is studied where the gluonic jets are identified with hadronic clusters. Of particular interest is the nature of the event structure as it changes from a balance by many clusters at small p_T to a preponderance of the two jet configurations at large p_T. Effects previously ascribed to a parton k_T are naturally reproduced in this approach because the production of all particles, not just a subsystem, is described.

There is an intimate connection between the production of a massive state of mass m and of a large p_T particle. At the most obvious level, the massive particle can decay to give particles of considerable transverse momentum ($p_T \leqslant m/2$). In a hard scattering approach, a parton from each incoming hadron can combine to make a massive system as discussed in Sections 4.2 and 4.4. This is a very similar mechanism to their scattering to produce large p_T jets. In a hadronic approach, the natural quantity to consider turns out to be the transverse mass $m_T = (m^2 + p_T^2)^{1/2}$ and this relates m and p_T dependences as discussed in Section 3.3. The massive systems that are of interest experimentally include the weak vector bosons $W^{\pm}$ and Z° and a dilepton pair ($\mu^+\mu^-$ or e^+e^-) of large invariant mass which is produced from a virtual massive photon. The relationship between the production of weak and electromagnetic systems of the same mass is, of course, given explicitly by a unified model of weak and electromagnetic interactions. This enables estimates of weak vector boson production to be made. The other class of massive system that is of considerable interest is that of hadrons which contain heavy quarks: the ψ family of $c\bar{c}$ mesons with mass above 3.1 GeV, the D family of $c\bar{q}$ mesons with mass above 1.9 GeV and possible states made of yet heavier quarks such as the Υ at 9.5 GeV. A QCD approach to the decay of the ψ meson is able to explain the narrow width since gluons with large momentum transfer are involved and these have smaller effective coupling. This gives encouragement that a parton model approach to ψ production should also be worth investigating. This is discussed in Section 4.4.

If an incoherent hard scattering process is responsible for the production of large p_T hadrons, then the production on a nuclear target should just be equal to the sum of the production on each individual nucleon. This gives a dependence on the nucleon number as $A^{1.0}$. Data indicate a dependence which rises faster than this (as much as $A^{1.3}$). Within a parton model approach there can be additional effects due to the extra virtual mesons which bind a large nucleus. These effects do not seem to explain the data satisfactorily. A multiple scattering approach is able to give an adequate description. These matters are discussed in Section 5.

There have been many reviews recently on theories of large p_T phenomena[84, 67, 46, 44, 78, 82, 40] which enable the reader to trace the full literature, and I shall thus give reference predominantly to recent work. Since I am aware that data quickly becomes superseded, I recommend a study of conference reviews to update information on the results of recent experiments.

2. SALIENT FEATURES OF DATA

A summary of data on large transverse momentum and on large mass production in hadronic collisions is presented. This will provide a framework for the discussion of theoretical models in Sections 3 and 4. Discussion of certain experimental results which are of particular relevance to specific models will be postponed to later sections.

2.1. Large transverse momentum

Inclusive spectra. The distribution of transverse momenta of particles produced in hadronic collisions was known to be approximately exponential at lower energies. The first evidence for a substantial departure from this behaviour came from the ISR experiments[18, 1, 8] which detected π production at large centre of mass angles in proton–proton collisions. They found an excess of events at larger transverse momentum (p_T) compared with an exponential behaviour and, moreover, this excess became relatively larger at higher energies. A compilation of data illustrating this effect is shown in Fig. 1. This observed rise with energy immediately introduces the question of what the asymptotic p_T dependence might be. This can be investigated by parametrizing the data at several energies and hence extrapolating to higher energies. A popular parametrization of the single particle-inclusive spectrum at fixed angle is to express the invariant cross-section as

$$E\frac{d_\sigma^3}{dp^3}=cp_T^{-n}f(x_T) \tag{2.1}$$

where $x_T=2p_T/\sqrt{s}$ (or p_T/p_T max may be used). A typical choice of functional form (in GeV units) for π production at 90° with $p_T>3$ GeV gives $n=8.6$ with $f(x_T)=\exp(-12.5x_T)$ and

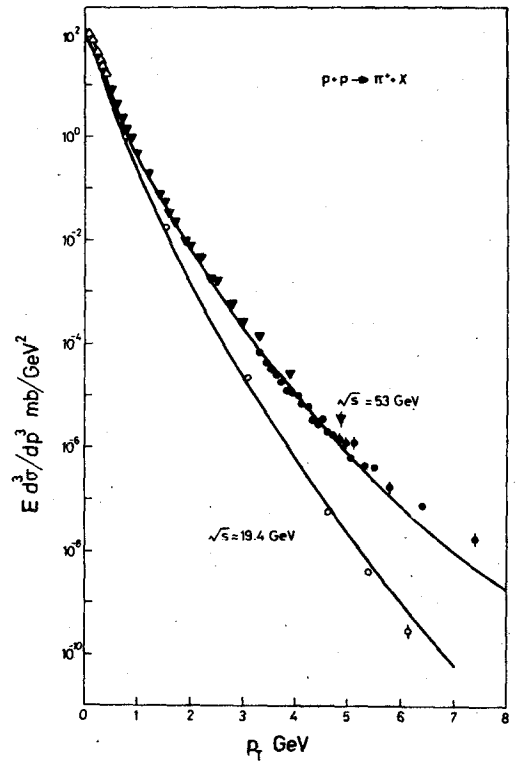

FIG. 1. The invariant inclusive π^+ production spectrum in pp collisions at 90° in the centre of mass and at total energy $\sqrt{s}$ as a function of the transverse momentum p_T. Data from refs. 3, 5, 20, and 51. The curves, which serve to guide the eye, are from ref. 76.

$C = 9.0\,\text{mb}$.[20] Other analyses of inclusive π production data also lead to a value of n of between 8 and 9.[3,5] Present data by no means necessitate an asymptotic inverse power law dependence on p_T, and forms such as $\exp(-b\sqrt{p_T})$ can also reproduce data.[90] Inclusive spectra for other particles than pions will be discussed in Section 2.2.

Event structure. Having established an interesting energy-dependent excess of inclusive production at large p_T, the next step is to study the nature of the events in which these large p_T particles are produced. Experiments were devised to trigger on a large p_T particle at a large centre of mass angle (usually at 90°) and then the associated produced particles were studied. The resulting picture emerged slowly but for clarity I shall describe the present consensus.[29,75,30,31,14]. Schematically this is illustrated in Fig. 2. The word jet is used to mean a group of particles travelling in a very similar direction. The presence of a dynamically significant jet is revealed by a large positive correlation among pairs of particles close in direction and thus close in rapidity. For particles of small transverse momentum ($\lesssim 0.3$ GeV) there is considerable uncertainty in assigning these to the away-side jet, the same side jet or the background.

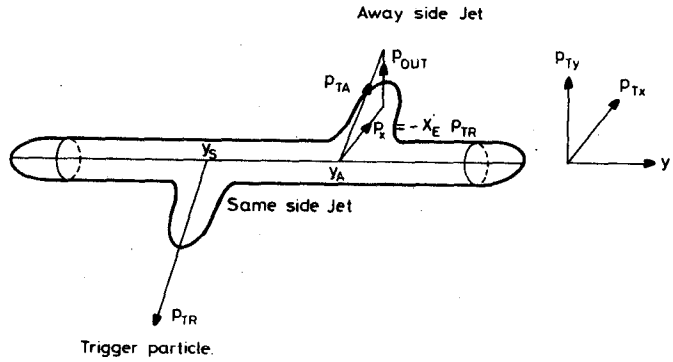

FIG. 2. A schematic representation of the distribution in longitudinal rapidity y and in transverse momentum p_T of a typical event with a trigger particle of large transverse momentum p_{TR}. The away-side transverse momentum p_{TA} is resolved into the component p_x in the plane containing the trigger particle and incoming hadrons, and the component p_{out} perpendicular to this plane.

Away-side jet. Event-by-event the away-side jet contains a group of particles of moderately large transverse momentum which are rather close to each other in rapidity (within 1 unit). This is illustrated in Fig. 3. However, in different events, the central rapidity of this away-side jet varies over most of the kinematically allowed range and, moreover, is substantially independent of the trigger rapidity. Thus the away-side distribution averaged over many events is very broad in rapidity; this is termed the away-side fan. The multiplicity in the away-side region increases approximately as $2(p_T^{-1})$ as the trigger momentum p_T increases.[4] The away-side jet is typically composed of many particles with relatively few having a large fraction of the total p_T; for example, $\sim 7\%$ of away-side jets have a charged particle with a transverse momentum greater than one-half of the net jet momentum.[30] In detail, the distribution of away-side particles with respect to a trigger particle is conventionally analysed in terms of x_e and p_{out} which are defined in Fig. 2. In naïve hard scattering models, the x_e and p_{out} distributions should be independent of the trigger momentum (i.e. should scale) and the average value of p_{out} should be ~ 0.3 GeV. Present

data with p_T of 2 to 4 GeV show substantial deviations from x_e scaling (see Fig. 4) and a broad p_{out} distribution with $\langle p_{out} \rangle \sim 0.6$ GeV.[30, 14]

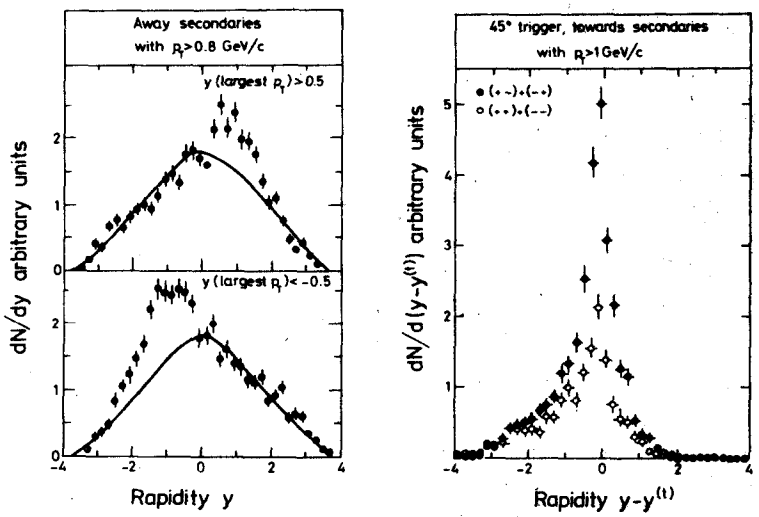

FIG. 3. The particle density in rapidity of secondary particles associated with a large p_T particle. On the away side, the rapidity of the largest p_T particle (with $p_T > 1.0$ GeV/c) is selected and then the density of other produced particles (with $p_T > 0.8$ GeV/c) is plotted. This shows a strong tendency for these secondaries to be produced at a rapidity close to that of the largest p_T particle. The curve is an estimate of the background expected. On the towards side (also called same or trigger side) the rapidity difference $y-y^{(t)}$ between the trigger particle and a secondary towards-side particle (with $p_T > 1$ GeV/c) is also shown to be peaked strongly at small values. Data are from the CCHK collaboration[30] with pp collisions at $\sqrt{s} = 53$ GeV and triggers at centre of mass angles of 45° and 20°.

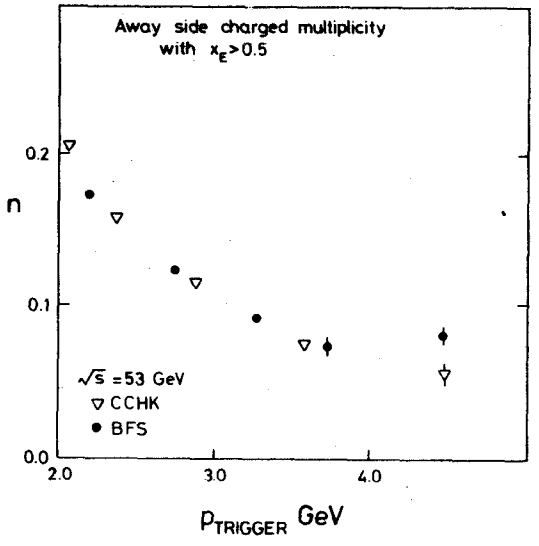

FIG. 4. The multiplicity of away-side charged particles with $x_E = |p_x/p_{TR}| > 0.5$. Data at $\sqrt{s} = 53$ GeV are from CCHK[30] and BFS.[14] The data from BFS are from the restricted region $|y| < 1$ and $|p_{out}| = 0.5$ GeV and have been renormalized arbitrarily. A decrease of this multiplicity with increasing trigger momentum is seen although an approach to a constant (as expected from scaling of the dn/dx_E distribution) is not ruled out.

Background particles. Also of interest are the beam and target fragments which are also illustrated in Fig. 2. Since the trigger particle and the away-side jet take away a substantial fraction of the initial total energy $\sqrt{s}$, one would expect the beam and target fragments to be less energetic with a large p_T trigger. One hypothesis is that the background of particles that accompanies the two jets (S and A) behaves as in a normal low p_T event but with the reduced energy of $(\sqrt{s}-E_S-E_A)$ and with a centre of mass momentum $-(p_S+p_A)$. This is in partial agreement with data for the leading particle distribution.[14] All of these fragments of the incoming particles also participate in the transverse-momentum balance and one finds an average transverse-momentum shift per particle of ~ 0.1 GeV in the away direction.[14] Thus the beam and target fragments can easily provide $\gtrsim 1$ GeV of transverse-momentum balance. This effect arises in parton models as a consequence of a broad parton transverse-momentum (k_T) distribution in a hadron.

Same-side jet. The trigger particle is accompanied by ~ 1 particle of smaller transverse momentum but close ($\lesssim \frac{1}{2}$ unit) in rapidity (see Fig. 3). This difference in the composition of the same side jet and the away-side jet arises from the effect of trigger bias. The inclusive cross-section to produce a jet of total transverse momentum p_T^J decreases with increasing p_T^J. It is thus favourable to produce a particle of a given p_T from a relatively rare decay of a jet which produces a substantial fragment ($p_T \sim 0.9 p_T^J$) rather than as a more typical fragment ($p_T \sim 0.3 p_T^J$) of a jet of considerably higher initial transverse momentum p_T^J which would thus have a much lower production rate. Data on the same-side jets indeed show that $p_T/p_T^J \sim 0.9$ on average[14].

Jet triggers. There is considerable theoretical interest in the inclusive production of jets. The experimental problem is to devise a trigger which selects the net transverse momentum of jets of particles close together in angle. Calorimeter triggers have been devised[15] and these register the energy of the charged particles and of most of the neutrals that enter. For particles produced at a lab. rapidity y_L, the energy in the laboratory frame is $E = m_T \cosh y_L$. Since the calorimeter is centred at a fixed angle θ_L in the lab. frame, then the rapidity of particles entering the calorimeter is related to θ_L by $p_T/(m_T \sinh y_L) = \tan\theta_L$. For high energies and large-angle production in the centre of mass system, y_L will be large, hence $\sinh y_L \simeq \cosh y_L$, and thus the energy available E is $p_T/\tan\theta_L$. The calorimeter energy sum is thus proportional to $\sum |p_T|$ and if the azimuthal angle subtended is small this will approximate $\sum p_T$. Another approach is to collect unbiased events in the central region and to analyse them subsequently (a software trigger) to look for jet-like combinations.[14,31]

The difficulty in interpreting such data lies in discriminating between a random fluctuation in the multiplicity density which can lead to several particles close in rapidity and in azimuth and an intrinsic jet signal. The average central region rapidity density is about 3 particles/rapidity unit. Thus in a range of $\Delta y = 1$ and of 30° in azimuth, only ~ 0.25 particles/event are expected. Among charged particles in this narrow cone there is little evidence for any extra jet effect on top of an uncorrelated emission of particles.[14] The FNAL experiment with a calorimeter trigger is able to register neutral energy as well as studying charge particles and they claim a significant jet signal. They obtain a jet to single particle inclusive cross-section ratio of $\gtrsim 100$ at $p_T \sim 3$ to 5 GeV.[15] The distribution of charged particles in the trigger jet is shown in Fig. 5.

Data on different large p_T triggers are consistent with each other if a large p_T jet is comprised completely of charge particles at a rate of $\sim 10\%$ and is comprised solely of a

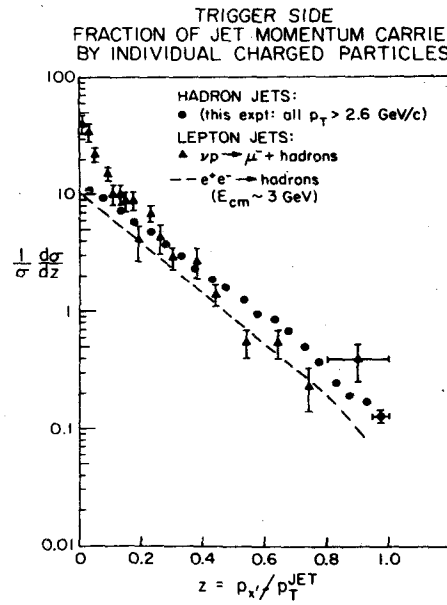

FIG. 5. Data from an inclusive jet trigger experiment on p-nucleus collisions at $p_{lab} = 150$ Gev/c.[15] The distribution of fractional transverse momentum z of a trigger-side particle to the triggered jet momentum is plotted. This is compared with data on the fractional momentum distribution of jets produced in neutrino interactions and in e^+e^- annihilation. A similar dependence is seen in each case.

single particle at a rate of $\lesssim 1\,\%$. Data on the composition of the away-side jet is consistent with this fraction of $\lesssim 1\,\%$ for single particles having $x_e \gtrsim 1$.[31] Indeed the away-side jet seen in single particle triggers has a very similar composition to both the away-side and same-side jets observed in jet triggered experiments.[15] Even with an inclusive jet trigger, there is a residual trigger bias since the net transverse momentum of the beam and target fragments, as discussed above, will be opposite to the trigger direction so that the away-side jet will have smaller transverse momentum than the triggered jet.

Charge ratios. There exist many data on the distribution and correlation of charge at large p_T. In pp collisions, the π^+/π^- inclusive production ratio is found to increase from ~ 1 to ~ 2 as p_T increases[5] as shown in Fig. 6. Another relevant ratio is the large p_T production of π° from $\pi^\pm p$ collisions compared to pp. This ratio is less than 1 at small x_T and rises to 2–3 at $x_T \sim 0.5$[34] as shown in Fig. 7. Concerning the charge distribution in individual events, the most striking result is that the charge composition of the away-side jet is independent of the charge or nature of the trigger particle (except for $\bar{p}$ or $\bar{K}$ triggers).[14] The charge ratio of leading particles in the away-side jet is also found to be ~ 2, independent of the trigger charge.[32,15]

2.2. Large mass

The average transverse momentum of heavier states is found to be larger than for π production. Put another way, at increasing transverse momentum, the fraction of heavy

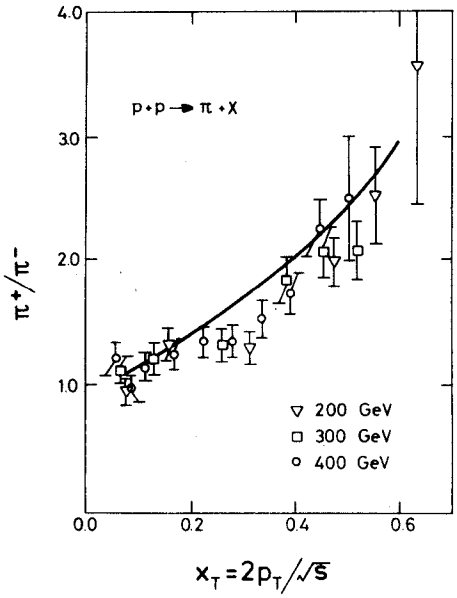

FIG. 6. The ratio of π^+ to π^- production in pp collisions at different lab. momenta, near 90° in the centre of mass and varying transverse momentum p_T.[5] The curve is the result of the model of ref. 42 based on a quark–quark scattering mechanism.

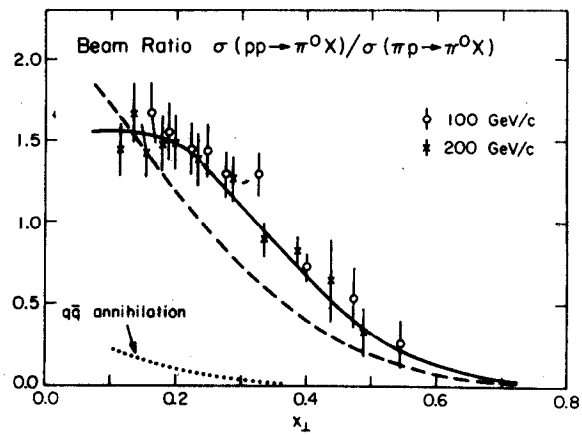

FIG. 7. The ratio of inclusive π° production near 90° in the centre of mass from pp collisions relative to πp collisions[34] for varying $x = 2p_T/\sqrt{s}$. The solid curve is the result of the model of ref. 42 based on quark–quark scattering and adjusting the pion structure function appropriately. The dashed curve is for a different pion structure function. The dotted curve is the expectation from using a $q\bar{q}$ annihilation subprocess.

states produced will be progressively enhanced. This effect can be discussed to advantage in terms of the transverse mass $m_T = (p_T^2 + m^2)^{1/2}$ of the state produced. It transpires that the m_T dependence of production spectra is fairly universal,[2] see also Fig. 8. For instance, the K^+/π^+ ratio[51,5] is found to be constant at ~ 0.5 when plotted versus m_T.[76] Data on the η°/π° ratio are likewise consistent with a constant value of 0.55 ± 0.11.[19] Data on the

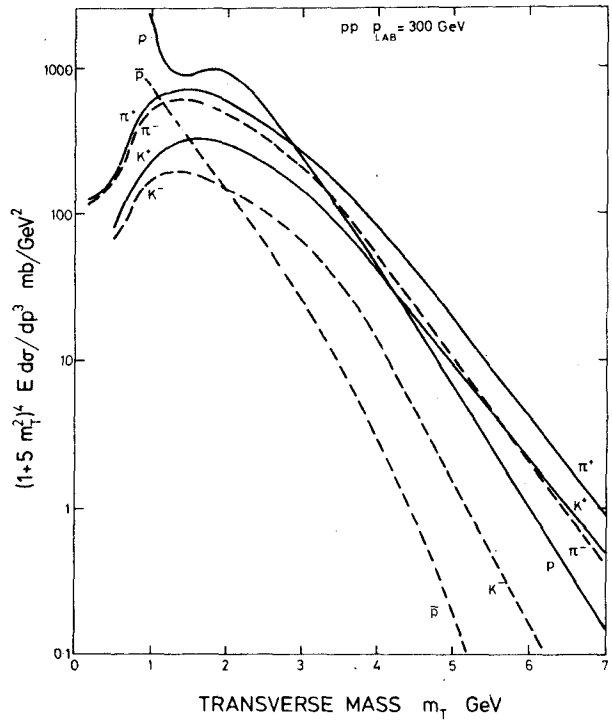

FIG. 8. The inclusive distribution of various particles at 90° in the centre of mass is plotted against the transverse mass $m_T=(p_T^2+m^2)^{1/2}$. A substantial part of the observed m_T dependence has been absorbed by multiplying the invariant inclusive cross-section by $(1+5m_T^2)^4$. Data are from refs. 51 and 5 and are at $p_{lab}=300$ GeV in pp collisions. The curves represent the trends of the experimental data points. The ratio of π^+/K^+ is seen to be constant at ~ 0.5 over the whole range of m_T.

$\bar{p}/\pi^-$ and K^-/π^- ratio in pp collisions[5] show a strong decrease at large m_T reflecting the difficulty of producing a $\bar{p}$ or K^- which arises in part from the need to produce an additional baryon or strange particle to conserve quantum numbers. A comparison of vector meson production including ψ production is shown in Fig. 9.[71]

Of particular interest are data on ψ and ψ' production at various energies and from various beams. The energy-dependent rise of the central region ψ production is well studied.[24] Data at lower energies show that ψ production from various beams is different with πp and $\bar{p}p$ being more productive than pp.[25] Concerning the event structure of ψ production, it is known that $\psi D\bar{D}$ is not the dominant process.[17] Whether radiative cascade decays from higher charmonium states (e.g. $\chi\rightarrow\psi\gamma$) are an important source of ψ particles is not established.

Another large mass system on which there is hadronic production data is dilepton pairs. In the higher mass region, the contributions to the dilepton spectrum from the decay of ψ, ψ' and Υ states should be considered separately. The continuum production, at invariant masses between these discrete states, can be considered as the production of a massive virtual photon. There is extensive data on the dependence of the production on the invariant dilepton mass m, the incident energy $\sqrt{s}$, and the longitudinal and transverse momentum of the dilepton pair. Data in the mass range of 7–11 GeV are consistent with a scaling form of

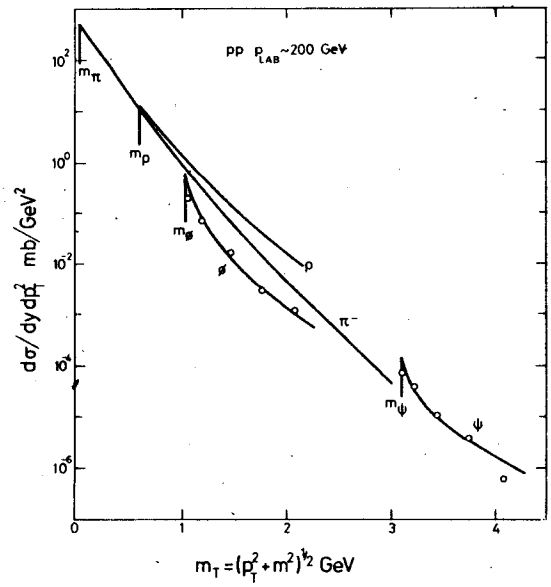

FIG. 9. The inclusive distribution of pions and of different vector mesons at 90° in the centre of mass is plotted against the transverse mass $m_T=(p_T^2+m^2)^{1/2}$. Data is from pp collisions at ~200 GeV.[3,16,51,71] The curves represent the trends of the experimental data points. For the vector mesons, the curves correspond to single exponentials in p_T and some data points are plotted to indicate the trend of the underlying data.

the production cross-section of $d\sigma/dm^2\,dy|_{y=0}=cm^{-4}\exp(-18m^2/s)$.[6] The transverse momentum dependence of dilepton production is of considerable interest. Data suggest that $\langle p_T\rangle$ increases with increasing m up to a constant value of ~1.3 GeV at $m>3$ GeV.[57,6,69] The $\langle p_T\rangle$ values for ψ and Υ production are found to be the same as those from the continuum regions on either side in mass m of the resonance peaks (see Fig. 10). A comparison of data with different beams shows that π-nucleon collisions are more productive than proton–nucleon collisions. The ratio of production from a π^+/π^- beam is less than one, except at $m\sim3$ GeV where ψ production dominates and hence the ratio is one from isospin invariance.[16]

3. HADRONIC MODELS

The first subsection contains a brief résumé of average p_T physics. This allows the subsequent discussion of extensions to larger p_T to be put in context.

3.1. Résumé of low p_T models

(*a*) *Data.* Before discussing theoretical models, a very condensed account of the salient features of typical high-energy multiparticle production is given.[45]

(i) *Multiplicity.* Many particles are produced on average and they are predominantly pions. The average multiplicity $\langle n\rangle$ depends on the energy available for particle production

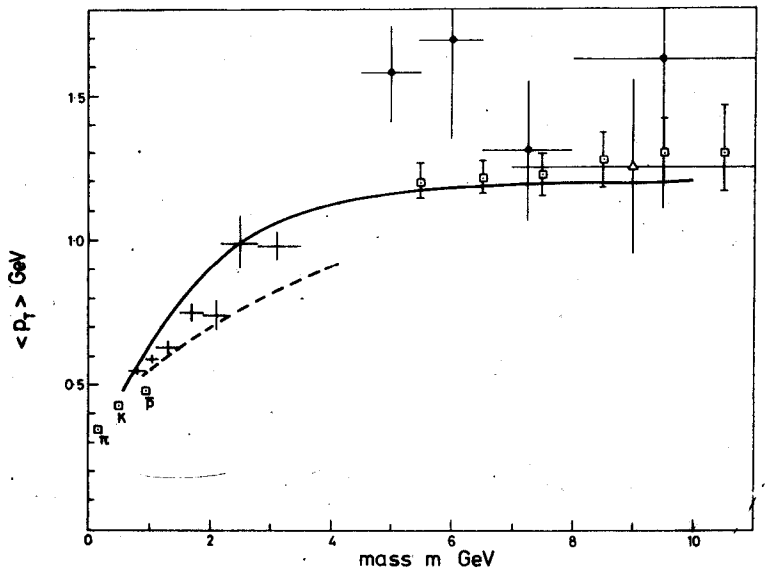

FIG. 10. The average transverse momentum of different systems of invariant mass M produced near 90° in the centre of mass in pp and p nucleus collisions at high energy ($\sqrt{s} \sim 20$ GeV). The data on π, K and $\bar{p}$ production are taken from ref. 83. The dashed curve gives the trend of data on the production of 4π and 6π systems as determined by ref. 86. The other points are for dilepton pair production from refs. 6, 16, 57 and 69. The solid curve represents the result of eqn. (3.7).

($\sqrt{s}$) but is broadly independent of the nature of the system that produces this energy. The traditional approximation is that the multiplicity distribution is a Poisson distribution and that $\langle n \rangle$ increases like $\ln s$. The multiplicity distribution is in fact broader than a Poisson distribution and roughly retains its shape with increasing energy when n is scaled by $\langle n \rangle$. The increase of $\langle n \rangle$ with energy is found to be faster than $\ln s$ and is consistent with a $\ln^2 s$ term included.[88]

(ii) *Limited p_T.* The average transverse momentum of pions is small ($\langle p_T \rangle \sim 0.35$ GeV) and is independent of the total energy. In detail, as a function of the centre of mass longitudinal momentum fraction $x = p_L/p_{\max} \simeq 2p_L/\sqrt{s}$, $\langle p_T \rangle$ shows a slight minimum at $x = 0$ (the seagull effect). As a function of the centre of mass rapidity y, however, $\langle p_T \rangle$ is rather constant with a maximum at $y = 0$. For small p_T, the p_T dependence is consistent with an exponential decrease with increasing m_T like $\exp(-7m_T)$.

(iii) *Central region.* In the central region (at fixed centre of mass rapidity y) the particle density dn/dy is traditionally considered to be a constant independent of the energy available $\sqrt{s}$ or of the centre of mass rapidity y. This is the central plateau. In detail, dn/dy increases slowly with total energy $\sqrt{s}$.[88] The y dependence of dn/dy shows a peak at $y = 0$ with a distribution that broadens (like $\ln \sqrt{s}$) with increasing energy. At $\sqrt{s} \sim 60$ GeV, $dn/dy \sim 3$ in the central region. In terms of x, the central region appears approximately exponential in $|x|$ with a peak at $x = 0$.

(iv) *Leading particles.* There are leading particles in the beam and target fragmentation regions which carry finite fractions x of the incident centre of mass longitudinal momentum in hadronic collisions. These leading particles may be considered as fragments of the